Residual Stresses in Amorphous Polymers

*Luigi Grassia, Alberto D'Amore**

The 2nd University of Naples-SUN, Dept. Aerospace and Mechanical Engineering, Via Roma 19, 80031 Aversa (CE), Italy
E-mail: alberto.damore@unina2.it

Summary: The origin of internal stresses in a polymeric component, subjected to an arbitrary cooling, will be described. The differential volume relaxation arising as a result of the different thermal history suffered by each body point was considered as the primary source of stresses build up. A numerical routine was developed accounting for the simultaneous stress relaxation processes and implemented within an Ansys® environment. The volume relaxation kinetics was modelled by using the four-parameter TNM (Tool-Narayanaswamy-Mohynian) phenomenological theory using the PVT (Pressure–Volume-Temperature) data obtained on a polystyrene sample. The numerical algorithm translates the specific volume theoretical predictions at each body point as applied non-mechanical loads acting on the component. Thermorheological complexity emerged due to coupling of volume and stress relaxation phenomena A linear dependence of Poisson's ratio on the tensile relaxation modulus was postulated. A quantitative predictions of time dependent stress distribution was realized for two specific test cases.

Keywords: residual stress; structural relaxation; viscoelasticity

1 Introduction

Residual stresses within a freely standing body are essentially associated with the mismatch of thermal expansion coefficient (and eventually the elastic properties) among the phases. Such condition is easily recognized when semi-crystalline polymers or composite materials are under concern. In fact, the different thermal histories suffered by each body point during the processing operations of semi-crystalline materials (due to the transient heat transfer phenomena) cause different structures (morphology and amount of crystalline phases) and consequently a variation of "local" thermo-elastic properties. In the same way, composite materials consist generally of inorganic fibers embedded in a polymeric matrix where either the expansion coefficients or the elastic properties of the constituent phases may differ by orders of magnitude.

In the above-cited examples, it is clear that, in principle, some order parameters can be invoked to describe the "local" structure of the materials (i.e. the grain size, the amount of

 DOI: 10.1002/masy.200551001

crystals, the volume fraction and the geometry of fibers an so on). On the contrary, amorphous monolithic materials (including the amorphous part of semi-crystalline polymers) are free of any "structure" and in general, they are regarded as homogeneous and isotropic materials. In such a case the internal stresses are, in fact, totally attributed to the volumetric fluctuations, associated with the kinetics of the glass transition, that lead to a resulting incomplete viscoelastic relaxation during solidification.

Residual stresses can play an important role in the structural integrity of a wide range of products: among the others, the dimensional stability and durability are the performance mostly affected by warping, anisotropic shrinkage and product flaw-induced residual stresses. The effects of temperature and time-dependent behavior of polymeric materials on residual stresses has been the subject of numerous investigations[1-13]. In this paper a numerical procedure is proposed to predict the residual stresses in freely standing objects taking into account the simultaneous structural and viscoelastic relaxations phenomena occurring under arbitrary thermal histories.

2 Structural Recovery in Glasses

Referring to Figure 1, when a glass forming material is cooled from the melt state, the glass transition is reveled by a change in the temperature dependence of any structure-sensitive property. The slope dP/dT (where P is the generic property) changes from the high value characteristic of the liquid to the low value characteristic of a glass. The glass transition temperature T_g is defined, in this work, as the intersection of the high and low temperature lines. Under isothermal conditions below T_g, (i.e. under out of equilibrium conditions) a spontaneous (time-dependent) evolution of each property is observed that as come to be referred to as structural relaxation. Hence it is necessary to define the thermodynamic "actual" state of the glass. This has been done historically in two ways. The most common is to conceive the glassy state as being defined by the absolute temperature T and by a structural parameter referred to as the fictive temperature, T_f[1]. The fictive temperature is defined by taking a point in the glassy state and drawing from it a line parallel to the glassy volume or enthalpy line until it intersects the equilibrium line. The abscissa of the point of intersection defines T_f. The other definition of the glassy state comes from the work of Kovacs et al.[2] and is defined in terms of departure from equilibrium, δ, that is defined as $(P-P_\infty)/P_\infty$ where the subscript ∞ denotes the equilibrium value of P. Clearly the isostructural state defined by T_f and by δ are related but not

identical. The distinction between them arises into models of kinetics of glassy recovery, namely the Tool-Narayanaswamy-Moynihan (TNM)[1,3,4]and the Kovacs-Aklonis-Hutchinson-Ramos (KAHR) models[2].

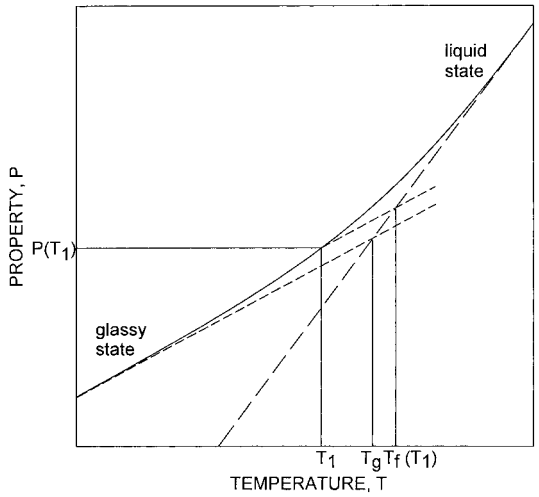

Figure 1. Schematic of generic property P vs temperature for glass-forming materials.

In this work we used the TNM model in which the evolution of T_f is described by the equations:

$$T_f = T - \int_{T_0}^{T} \exp\left[-\left(\int_0 \frac{dt'}{\tau}\right)^{\beta}\right] \qquad (1)$$

$$\tau = A \cdot \exp\left[\frac{x\Delta h}{RT} + \frac{(1-x)\Delta h}{RT_f}\right] \qquad (2)$$

where τ is the structural relaxation time, A is a constant (pre-exponential factor), Δh is the characteristic activation energy, x the partitioning parameter ($0<x<1$) that defines the degree of nonlinearity, β is the shape parameter describing the stretching of the relaxation function, and R is the gas constant. The model parameters for amorphous PS were obtained minimizing the sum of squared differences between the values from PVT measurements and those predicted solving equations 1 and 2 with a home-made FORTRAN program[5]. The polystyrene resin was a commercial product, supplied in form of powder by Aldrich, with $M_N = 92{,}000$ and $M_W = 220{,}000\ \ g/mol$.

The found optimum set of parameters (lnA=-276 min., $\Delta h/R=1.03x10^5$K, x=0.9 and β=0.272) [5] can be utilized to predict the structural relaxation under any given thermal history.

3 Viscoelasticity

Linear viscoelasticity is assumed. A discrete spectrum of relaxation times is utilized to describe both deviatoric and volumetric part of the stress-strain relationship. Shear stress relaxation data were obtained under isothermal conditions in a range of temperature above the glass transition in order to construct a master curve for the melt state that is reported elsewhere[5]. A plot of the relaxation time shift factors shows that their temperature dependence is well described by the WLF equation with c_1=7.04, c_2=89.8deg at a reference temperature of 140°C.

The time dependence of the bulk modulus was obtained assuming a linear dependence of Poisson's ratio on tensile relaxation modulus:

$$\frac{E(t)-E_\infty}{E_0-E_\infty}=1-\frac{\nu(t)-\nu_0}{\nu_\infty-E_0} \qquad (3)$$

The modeling procedure to obtain the bulk relaxation modulus from this hypothesis is described in details elsewhere[5]. Here we only empathize that with this simple assumption the principal relaxation time for the bulk modulus is three order of magnitude larger than that corresponding to the shear modulus. Below T_g, relaxation times depend on glassy structure. This is well described in the so-called memory or crossover experiment[6]. The parameter describing, together with the temperature, the structure in the actual glassy state is T_f , Therefore the fictive temperature is introduced in the expression of the mechanical relaxation shift factors, $a(T,T_f)$, as follows:

$$\ln\left[a\left(T,T_f\right)\right]=\frac{\Delta h'}{R}\left(\frac{1}{T_{ref}}-\frac{x}{T}-\frac{1-x}{T_f}\right) \qquad (4)$$

where Δh' is activation energy of mechanical relaxation phenomena and is, in general, different from the value calculated from the volumetric relaxation data. The parameter "x" maintains the same significance described previously in the framework of TNM theory. It represents now the relative contributions of T and T_f to the evolving structure-dependent mechanical shift factors. Δh' was obtained fitting the shift factors for the shear relaxation modulus with an Arrhenius-type equation (see Figure 2) in a narrow range of temperature above T_g. The $\Delta h'/R$ best fit value is $3.91x10^4$ K.

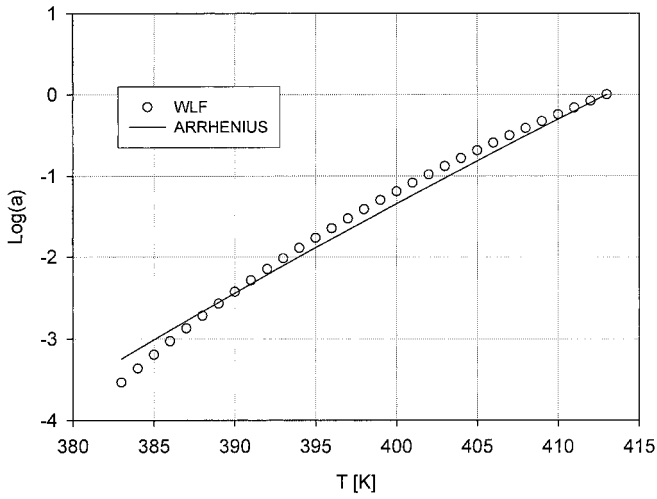

Figure 2. WLF and Arrhenius temperature dependence of the mechanical relaxation shift factors.

According to this approach a dramatic view of structure-dependent shift factors is shown in Figure 3, where the temperature dependence of the calculated shift-factors, for samples cooled from 413 K to 293 K at different cooling rates, is reported. It can be observed that as the cooling rate increases the shift factors decrease, according to their structure dependence. This is in agreement with the experimental evidences reported frequently in literature[7, 8].

4 Modeling Strategy

The residual stresses distribution induced in a polystyrene sample of given geometry, subjected to arbitrary thermal histories, were evaluated developing a numerical routine coupling a structural and a thermal finite element analysis. In order to start the numerical procedure, a preliminary determination of the temperature distribution vs. time was performed assuming that the stress distribution do not affect the heat transfer problem[9]; the results from this calculation in terms of a three-dimensional temperature distribution have been provided to the numerical routine, based on the optimized parameters of the TNM theory, and allows the knowledge of time dependence of specific volume at each

body point. Then the incremental change in growth (volumetric) strain at each body point can be calculated at a given time as follows:

$$\varepsilon^{th}\left(t,\bar{X}\right)=\frac{v\left(t,\bar{X}\right)-v\left(0,\bar{X}\right)}{v\left(0,\bar{X}\right)} \qquad (5)$$

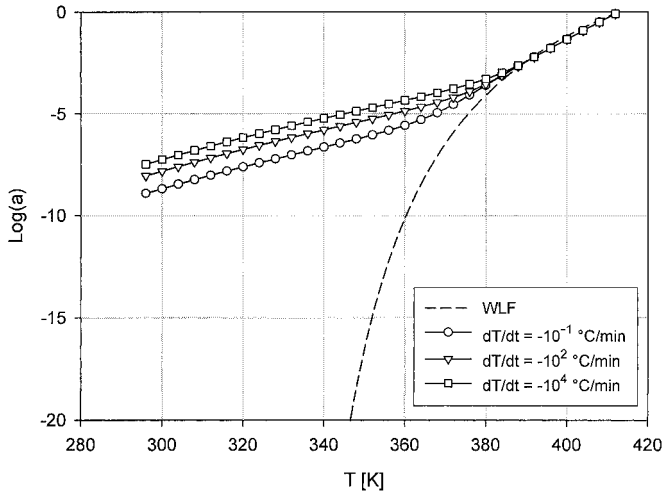

Figure 3. Calculated time-temperature-fictive temperature shift function vs. temperature at different cooling rate dT/dt. The dashed line represents the WLF dependence of the mechanical shift factor.

Finally, imposing the congruent displacement and equilibrium conditions the stresses evolution can be calculated. The numerical strategy is summarized in Figure 4.

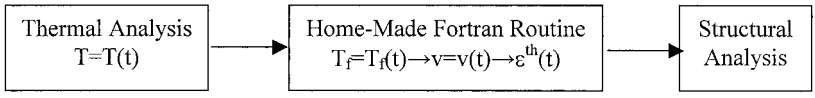

Figure 4. Numerical Strategy Scheme.

In the thermal analysis the thermal diffusivity has been assumed constant: calculations of Goslinga[9] showed that the errors involved under these hypotheses are quite small. The ambient temperature T_∞ and the global convective heat transfer coefficient H have been assumed constant during cooling; the initial temperature, T_0, has been assumed uniform and all the external surfaces of the sample have been considered involved in the heat transfer phenomena.

The evaluation of residual stresses will be carried out in two different test cases:

1. A cylindrically shaped polystyrene sample that undergoes a complex thermal history reported in Figure 5 with T_∞=20°C and T_0=140°C. A parametric analysis on the radial cylinder dimension R_0 and T_{int} (T_{int} is the intermediate temperature) is performed (with 1mm≤R_0≤50mm and 95°C≤T_{int}≤115°C, respectively). The cylinder length L is 20 times R_0. The global convective heat transfer coefficient has been assumed equal to 1000W/m^{2}K (a characteristic value of natural convection in water). Only a quarter of an axial section of the cylinder has been FE modelled due to the axial and transversal symmetries of the structure.
2. A polystyrene plate that undergoes a simple quenching from T_0=140°C to T_∞=20°C characterized by asymmetrical thermal boundary conditions schematically reported in Figure 6 together with the plate dimensions.

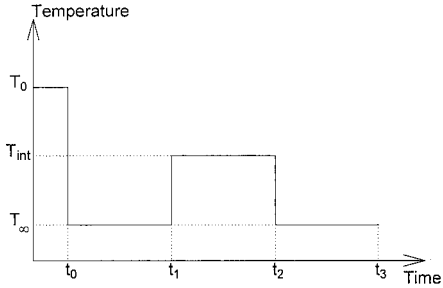

Figure 5. Schematic of thermal history in the test case 1.

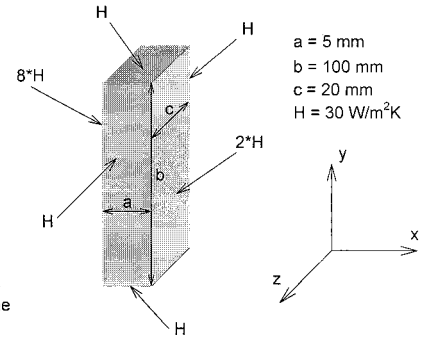

Figure 6. Thermal boundary conditions and plate dimensions in test case 2.

5 Results and Discussions

Upon cooling, the temperature decreases more rapidly at the surface than in the inner part. A thermal gradient appears in the thickness that implies transient and residual stresses.

The surface contraction occurs rapidly leading to a compression state in the core and a tensile state at the surface. When the temperature is below the transition range, contraction at the surface slows down while the core, still liquid, continues to cool and contract until its temperature is far below the glass transition. In absence of thermal gradients at temperature far below T_g (i.e. room Temperature for polystyrene) the surface is in compression and the core in tension. This general behaviour can be attributed to both the viscoelastic nature of the polymer and the effects of structural relaxation. Our numerical

approach implicitly takes into account the two phenomena acting simultaneously through the (volumetric) fictive temperature. The use of the same fictive temperature function for the determination of volume relaxation behaviour and for the implementation of the viscoelastic shift function simplifies the problem, though, at moment, it represents the best way to manage it.

5.1 Test Case 1: Polystyrene Cylinder

Figure 7 displays the shear relaxation modulus predictions vs. temperature during the first cooling (t_0,t_1) at different value of the dimensionless radial position.

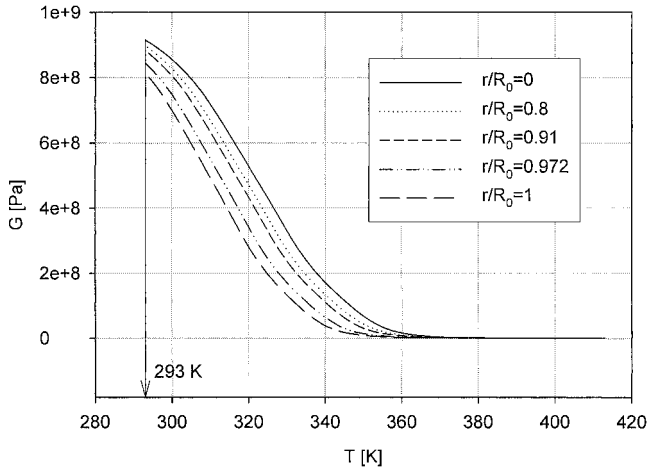

Figure 7. Calculated shear relaxation modulus vs. temperature at different value of r/R_0. r is the radial coordinate and R_0=5mm.

Because the cooling is faster at the surface, T_f increases with the radial coordinate. Accordingly the shear relaxation modulus, G, decreases. In Figure 8 we report , for clarity, the calculated shear modulus vs. the specific volume at 293 K. It can be observed a linear dependence of the shear modulus with the specific volume (G is structure-dependent) that reproduces some experimental evidences documented in literature[10].

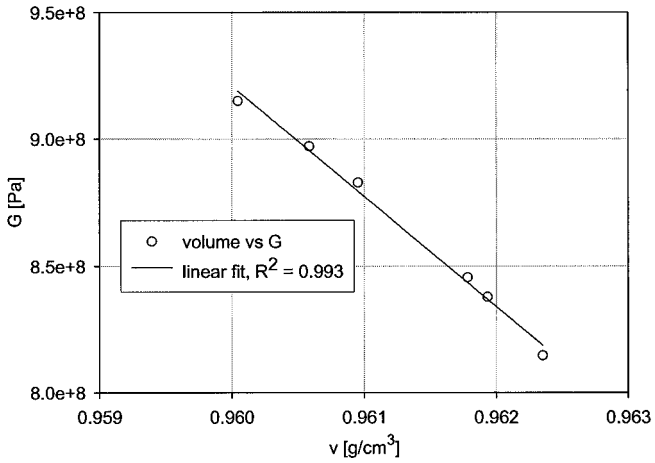

Figure 8. Shear modulus versus specific volume at 293 K in the case of R_0=5mm.

Figure 9 shows the residual stresses vs. the dimensionless radial position at time t_1=480s, when the thermal equilibrium is reached, in the case of R_0=5mm.

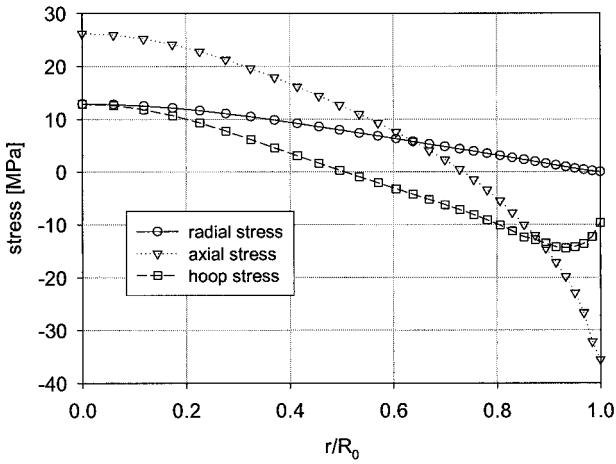

Figure 9. Residual stresses vs. r/R_0, R_0=5mm.

A parametric analysis can also carried out in order to predict the influence of radial dimensions on the residual stresses. In Figure 10 a plot of axial and hoop stress at the surface and at the center line as function of Biot number is reported.

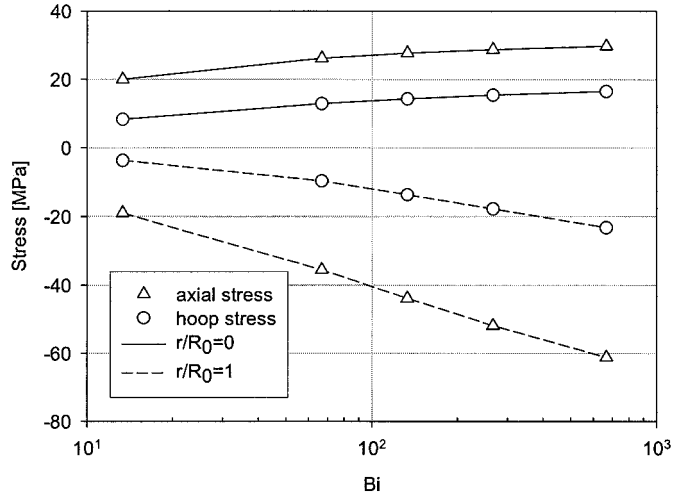

Figure 10. Residual stresses vs. Biot number for a polystyrene cylinder quenched from T_0 to T_∞.

In Figure 11 the axial stress shows a quasi-linear dependence on ln(Bi).

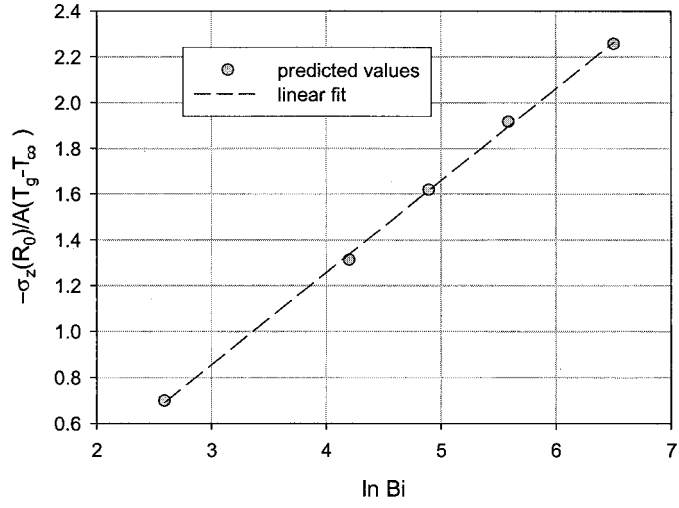

Figure 11. Dimensionless axial residual stresses vs. ln Biot number for a polystyrene cylinder quenched from T_0 to T_∞.

This is in agreement with Struik (1) prediction, but a linear fitting of dimensionless axial stress $\frac{-\sigma_z(R_0,\infty)}{A(T_g - T_\infty)}$ vs. ln(Bi) (with E_g = 3000 MPa, α_g=7x10^{-5} K^{-1} and ν_g = 0.38 A = $\alpha_g E_g/(1-\nu_g)$=0.34 MPa/K), shows in our case a slope of 0.4 which is little lower than the Struik predicted value of 0.5. Figure 12 shows the parametric time evolution of the hoop stress at the centre of the cylinder as function of the following thermal history also illustrated in Figure 6:

- reheating (up-quench) the sample at $t \geq t_1$ to different value of the T_{int} (including Temperatures higher than T_g)
- holding the temperature constant for a given time interval (t_2-t_1)
- quenching down to room temperature at t= t_2.

A strong increase of hoop stress is revealed in correspondence of t_1 and t_2 even this stresses are relaxed later.

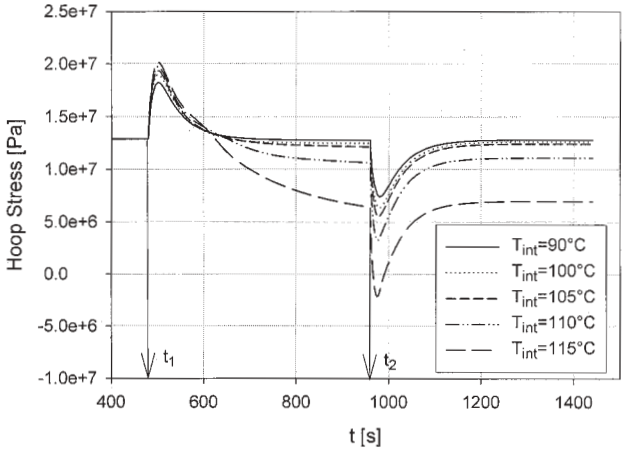

Figure 12. Hoop stress vs. time ($t \geq t_1$) at r/R_0=0.

In order to clarify the effect of the complex thermal history upon the residual stress, in Figure 13 we report the ratio the of residual stresses at the end of the second cooling (at t = t_3) and at the end of the first cooling (at t = t_1) vs. T_{int}. We observe a reduction of residual stresses with increasing the T_{int} value.

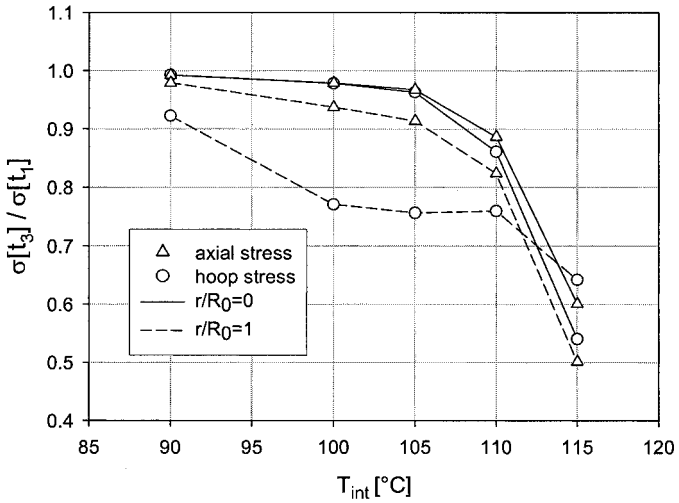

Figure 13. Ratio of residual stress calculate at t_1 and at t_3 vs. T_{int} for a polystyrene cylinder with R_0=5mm.

This is due to two combined effects that can be better clarified by looking at Figure 14 were the calculated volume relaxation behaviours at the surface and at the centre of the cylinder are reported as function of temperature following the thermal history reported in Figure 5 with T_{int}=100°C. The two effects can be summarized as follows:

a) It can be recognized that at the end of the first cooling the difference between the volume at the inner part and at the surface of the cylinder is (v_A-v_B) while it attains a lower value (v_B-v_C) at the end of the second cooling. Therefore the effect of such complex thermal history is to reduce the overall volume difference inside the cylinder and, accordingly, the contribution of structural relaxation on residual stresses should decrease.

b) Reheating to a temperature T_{int} induces a partial relaxation of the residual stresses accumulated after the first cooling.

A more complex puzzle (although fulfilling our physical expectations) emerges from Figure 15 where T_f values at r/R_0=0.8 at time t_2 and t_3 as function of the temperature, T_{int}, are reported (for the sake of clarity, it is also reported the fictive temperature at time t_1).

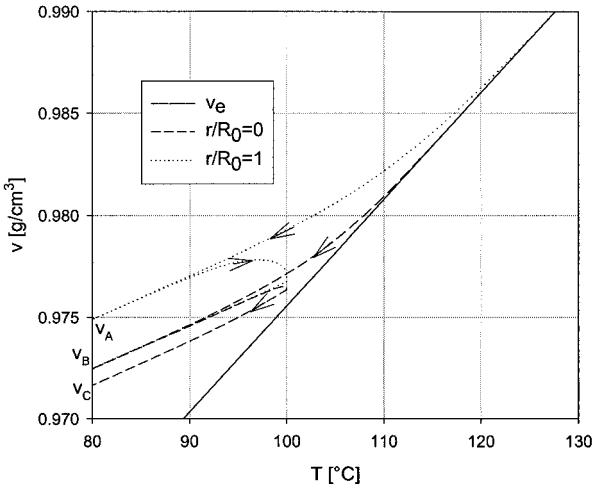

Figure 14. Specific volume calculated from TNM model during the complex thermal history with T_{int}=100°C at the centre and on the surface of the cylinder

The $T_f(t_3)$ *is not* a monotonic function of T_{int} and therefore the reduction of residual stresses due to structural relaxation will follow the same trend. Moreover, with increasing T_{int}, T_f (t_3) merge $T_f(t_1)$ and $T_f(t_2)$= T_{int}, so that the volume profile inside the cylinder predicted by the TNM model is the same at t_1 and at t_3 for T_{int}=115°C while Figure 12 shows a monotonic decreasing of the stress ratio with T_{int}. In all we have, for the same volume (TNM predicted at a given radial position at two different times), two different value of residual stresses. This is simply the effect of the viscoelastic contribution to the residual stress build-up.

5.2 Test Case 2: Polystyrene Plate

The left part of Figure 16 displays the deformed shape of the polystyrene plate while the residual stress profile is reported on the right. Both the residual stress profile and the deformed shape are asymmetrical due to the asymmetrical boundary conditions.

Conclusions

A numerical procedure was developed in order to predict residual stresses in freely standing bodies subjected to arbitrary thermal histories. The three-dimensional predictions of volume relaxation based on TNM phenomenological theory were transformed to local

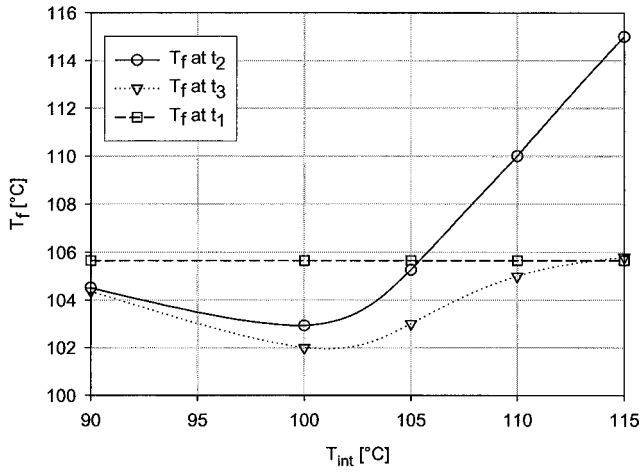

Figure 15. Fictive temperature at t_1, t_2, and t_3 vs. the T_{int} at $r/R_0=0.8$, $R_0=5mm$.

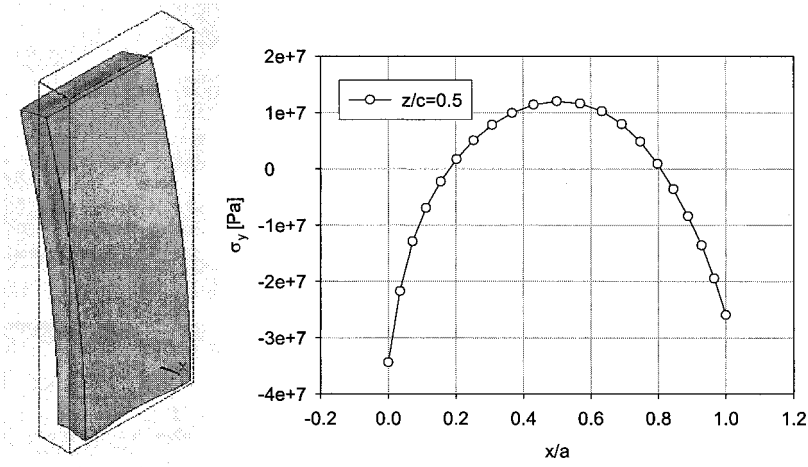

Figure 16. On the left: deformed shape of the polystyrene plate; on the right: σ_y stress vs. the dimensionless coordinate in the x direction for z/c=0.5 and y/b=0 for the polystyrene plate.

deformations. Stress relaxation emerging from point to point differential volume relaxations were modelled by using time-temperature-fictive temperature dependent shift factors. The dependence of shift factors on fictive temperature represents the way the volume relaxation influences stress relaxation.. A 3D structural analysis allowed for

reasonable residual stresses predictions. To date the analysis presented suffers the following approximations and/or assumptions:

1. The (subtle) way the stress affects the volume relaxation is not reported. This effects was never accounted for (at least explicitly) in any of the phenomenological theories for structural relaxation. Our recent modelling approach overcomes this shortcoming and the data presented here will be published elsewhere with such corrections.

2. In absence of bulk modulus data it was postulated a linear dependence of Poisson's ratio on tensile relaxation modulus. This assumption reflects the fact that relaxation functions span over several decades of time over which tensile modulus relaxes 4 to 5 orders of magnitude while Poisson's ratio relaxation function is confined between very narrow values (the unrelaxed glassy and the relaxed rubbery values are close to 0.3 and 0.5, respectively).

[1] O.S. Narayanaswamy; J Am Ceram Soc, 54, 491, **1971**
[2] A. J. Kovacs, J. J. Aklonis, J. M. Hutchinson, A. R. Ramos, Journal of Polymer Science: Polymer Physics, Vol. 17 1097-1162, **1979**
[3] C. T. Moynihan, A. J. Easteal, M. A. DeBolt, J Am Ceram Soc, 59, 12-16, **1976**.
[4] M. A. DeBolt, A. J. Easteal, P. B. Macedo C. T. Moynihan, J Am Ceram Soc, 59, 16-21, **1976**.
[5] A. D'Amore, M. Zarrelli, L. Grassia, F. Caputo,.Composites Part A-Applied Science and Manufacturing, **2005**. in press.
[6] C. A. Angell, K. L. Ngai, G. B. McKenna, P. F. McMillan, S. W. Martin, 88, **2000**, pp 3133-3157
[7] Y. Yang, A. D'Amore, Y. Di, L. Nicolais, B. Li, Journal of Applied Polymer Scienc, Vol. 59, 1159-1166, **1996**
[8] M. L. Carrada, G. B. McKenna, "Physical Aging of Amorphous PEN: Isothermal, Isochronal and Isostructural Results", Macromolecules, **2000**, 33, 3065-3076
[9] L.C.E. Struik "Internal Stresses, Dimensional Stabilities and Molecular Orientations in Plastics", John Wiley and Sons Ltd. Chichester, England 1990.
[10] A. D'Amore, A. Pompo, L. Nicolais, Makromol. Chem., Macromol. Symp. 68, 203-212, **1993**
[11] G. Sherer, "Relaxation in Glass and Composites", **1986**, Wiley, N.Y
[12] S. Matsuoka, "Relaxation Phenomena in Polymers", **1992**, Hanser, Munich
[13] L.C.E. Struik, "Physical Aging in Amorphous Polymers and Other Materials", **1978**, Elsevier, Amsterdam